

materials can be prepared with zeolite coatings having thicknesses of tenths of a micron to over a millimeter in thickness depending on the particular synthesis conditions. The films are very stable toward mechanical, chemical, and thermal treatments. A reviewer has suggested that a stirred gel could be used to eliminate gradients during crystallization. This is the focus of current efforts. The chemical composition of the zeolites can be altered by ion-exchange procedures. It is likely that other synthetic procedures like adsorption, sublimation, and incipient wetness can be used to further alter the chemical compositions of these systems. Spectroscopic studies have shown that these zeolites are crystalline and homogeneous. Finally, it appears that there are several exciting possibilities for the use of such materials in the areas of catalysis, electrochemistry,²⁴ photochemistry, and semiconductor

devices.

Acknowledgment. First attempts to make zeolite thin films were initiated in L. R. Faulkner's lab, and we thank him for inspiration and ideas in this area. Helpful discussions with Lennox E. Iton of Argonne National Labs and Professor John Tanaka of the University of Connecticut are gratefully acknowledged. We thank Professor Leo Herbette of the University of Connecticut Health Center for making the synchrotron XRD measurements and Elsie Matthews of Biopolymers, Inc. for conducting the 180° peel strength measurements. Support for this research was from the University of Connecticut Research Foundation and the State of Connecticut Department of Higher Education through the High Technology Grant award program.

Hydrothermal Synthesis and Single-Crystal Structural Characterization of $V_2O_4(C_6H_5AsO_3H) \cdot H_2O$

Guohe Huan,* Jack W. Johnson,* and Allan J. Jacobson

Corporate Research Laboratories, Exxon Research & Engineering Company,
Annandale, New Jersey 08801

Joseph S. Merola

Department of Chemistry, Virginia Polytechnic and State University,
Blacksburg, Virginia 24061

Received June 12, 1990

The layered compound $V_2O_4(C_6H_5AsO_3H) \cdot H_2O$ has been prepared by hydrothermal synthesis and characterized by single-crystal X-ray diffraction. The structure is monoclinic, space group $P2_1/c$ (No. 14) with $a = 12.074$ (4) Å, $b = 9.574$ (3) Å, $c = 9.872$ (2) Å, $\beta = 107.63$ (2)°, and $Z = 4$ and is formed of undulating layers of vanadium, oxygen, and arsenic atoms with phenyl groups directed into the interlayer space. The phenyl groups from adjacent layers interpenetrate to form a monolayer of organic groups between the inorganic sheets, resulting in a layer repeat distance (d_{100}) of 11.507 (4) Å. The layers contain edge-shared pairs of $V^{5+}O_5$ square pyramids connected through corners to $V^{4+}O_6$ octahedra. The phenylarsonate moiety includes a terminal hydroxyl group that is hydrogen bonded to an oxygen atom of the vanadium oxide framework. The magnetic susceptibility displayed by the new compound follows the Curie-Weiss law in the temperature range 50–350 K, with reduced susceptibility due to antiferromagnetic coupling at temperatures below 50 K.

Introduction

Divalent metal phenylphosphonates and phenylarsonates $MC_6H_5RO_3 \cdot xH_2O$ (M = divalent metal, $R = P$ or As , and $x = 0, 0.5$, and 1) have been known for more than a decade.^{1,2} Although no single crystals suitable for structure determination were available, the morphology, color, powder X-ray diffraction patterns, and bulk magnetic properties indicated that these compounds belonged to an isomorphous series with structures in which layers consisting of octahedrally coordinated metal ions linked by multibridging acid groups are held together by weak van der Waals forces.² The structure of $MnC_6H_5PO_3 \cdot H_2O$ was reported recently.³ It consists of roughly coplanar

layers of manganese atoms coordinated by phenylphosphonate groups arranged above and below the plane of the manganese atoms and can be described as $MnO_{1/2}O_{4/3}(H_2O)_{1/1}C_6H_5PO_{1/2}O_{2/3}$. Each Mn atom is octahedrally coordinated by five phosphonate oxygen atoms and one water molecule. $ZnC_6H_5PO_3 \cdot H_2O$ is essentially isostructural⁴ with the Mn analogue. Microcrystalline $VOC_6H_5PO_3 \cdot 2H_2O$ was prepared in this laboratory⁵ by refluxing phenylphosphonic acid with V_2O_5 in 95% ethanol/water. The proposed structure can be described as $VO_{1/1}O_{3/2}(H_2O)_{2/1}C_6H_5PO_{3/2}$ and is analogous to that of the mineral newberyite,⁶ $MgHPO_4 \cdot 3H_2O$. Very recently, we have prepared single crystals of $VOC_6H_5PO_3 \cdot H_2O$ by

(1) Sandhu, S. S.; Sandhu, G. K. *J. Inorg. Nucl. Chem.* 1972, 34, 2249–2253.

(2) Cunningham, D.; Hennelly, P. J. D.; Deeney, T. *Inorg. Chim. Acta* 1979, 37, 95–102.

(3) Cao, G.; Lee, H.; Lynch, V. M.; Mallouk, T. E. *Inorg. Chem.* 1988, 27, 2781–2785.

(4) Martin, K.; Squattrito, P. J.; Clearfield, A. *Inorg. Chim. Acta* 1989, 155, 7–9.

(5) Johnson, J. W.; Jacobson, A. J.; Brody, J. F.; Lewandowski, J. T. *Inorg. Chem.* 1984, 23, 3842–3843.

(6) Sutor, D. J. *Acta Crystallogr.* 1967, 23, 418–422. Abbona, F.; Boistelle, R.; Haser, R. *Acta Crystallogr.* 1979, B35, 2514–2518.

hydrothermally reacting phenylphosphonic acid with V_2O_3 and determined its structure by single-crystal X-ray diffraction.⁷ The structure, $VO_{5/2}(H_2O)_{1/1}C_6H_5PO_3/2$, consists of layers of corner-sharing VO_6 octahedra and $C_6H_5PO_3$ tetrahedra. Within one layer, alternating short and long V–O bonds form chains running along the *b* axis. The phenyl groups extend out from both sides of the oxide layer, resulting in a layer repeat distance of 14.14 (2) Å. In a parallel study of the hydrothermal synthesis of arsenic analogues of the phenylphosphonates, two phases have been isolated with V/As ratios of 1 and 2. Single crystals of the compound $V_2O_4(C_6H_5AsO_3H) \cdot H_2O$ were obtained, and its synthesis, structure, and magnetic properties are described in this paper.

Experimental Section

Synthesis. The synthesis of vanadium phenylarsonates was investigated by reaction of $C_6H_5AsO_3H_2$ (Alfa) with V_2O_3 (Alfa) under hydrothermal conditions. Typically, the reactants were placed in a 23-mL Teflon-lined autoclave (Parr Instruments), and distilled water was added to give a fill level of 80%. The reaction vessel was maintained at 200 °C and autogenous pressure for 5 days. Reaction mixtures with V/As ratios of 0.33, 0.67, 1.00, and 1.25 were all heated under the same conditions. In the recently reported synthesis of $VOC_6H_5PO_3 \cdot H_2O$,⁷ the optimum conditions corresponded to V/P = 0.67. However, in the arsenic system, single phases were obtained only at reactant ratios of 1.25 and 0.33. At the reactant ratio V/As = 0.33, a compound was formed with morphology consisting of very fine needles and which by elemental analysis corresponded to the composition $VOC_6H_5AsO_3 \cdot 2H_2O$ (Galbraith Laboratories, Inc. Found: C, 23.70%; H, 2.90%; V, 16.93%; As, 25.81%. Calculated for $C_6H_5VAsO_6$: C, 23.78%; H, 2.98%; V, 16.81%; As, 24.72%). Thermogravimetric analysis (TGA) confirmed the presence of the two water molecules that are lost on heating in two steps with maximum rates at 130 and 245 °C. The presence of two steps in the TGA suggests that water molecules are coordinated to vanadium atoms in both cis and trans positions as observed in the vanadium phenylphosphonate dihydrate. However, the powder X-ray diffraction pattern of the phenylarsonate phase is more complex and cannot be indexed on the basis of a layered structure analogous to that of the phenylphosphonate compound. A structural study of this phase will require single crystals larger than those currently available.

The optimum reactant ratio (0.646 g of $C_6H_5AsO_3H_2$ and 0.300 g of V_2O_3) for the synthesis of the second phase was V/As = 1.25. Black needle-shaped crystals were formed (0.52 g, 67.5% yield based on V) with a composition $V_2O_4(C_6H_5AsO_3H) \cdot H_2O$. These were filtered, washed several times with distilled water, and air dried. Chemical analysis gave the following: C, 18.76%; H, 2.05%; V, 27.29%; As, 19.86%. Calculated for $C_6H_5V_2AsO_8$: C, 18.72%; H, 2.09%; V, 26.47%; As, 19.66%.

The vanadium oxidation state in $V_2O_4(C_6H_5AsO_3H) \cdot H_2O$ was determined by redox titration. Samples were dissolved in 1 M sulfuric acid. A known excess of cerium(IV) ammonium nitrate was added to the vanadium solution to oxidize all the vanadium ions to the pentavalent state. The total vanadium content and the average vanadium oxidation state were determined by potentiometric titration using a standard solution of ferrous ammonium sulfate. The results gave $V^{4+}/V^{5+} = 1.04 \pm 0.02$. The total vanadium content was 26.75%, in agreement with the results of the elemental analysis.

Magnetic susceptibility measurements were made from 10 to 350 K using a George Associates Faraday magnetometer with an applied magnetic field of 6.2 kG.

Infrared spectra were recorded on samples in KBr disks by using a Mattson Polaris spectrometer.

X-ray Crystallography. Crystal data: monoclinic, $P2_1/c$ (No. 14), $a = 12.074$ (4) Å, $b = 9.574$ (3) Å, $c = 9.872$ (2) Å, $\beta = 107.63$ (2)°, $Z = 4$, $D(\text{calc}) = 2.351$ g/cm³. A Nicolet R3m/V diffractometer, with Mo $K\alpha$ radiation ($\lambda = 0.71069$ Å) and a graphite

Table I. Atomic Coordinates ($\times 10^4$) and Equivalent Isotropic Displacement Coefficients ($\text{\AA}^2 \times 10^3$)

	<i>x</i>	<i>y</i>	<i>z</i>	<i>U</i> (eq) ^a
As(1)	7379 (1)	1484 (1)	5439 (1)	16 (1)
V(1)	5462 (1)	2213 (1)	2428 (1)	15 (1)
V(2)	3862 (1)	-444 (1)	121 (1)	14 (1)
O(1)	2850 (3)	648 (3)	-502 (3)	27 (1)
O(2)	7400 (3)	107 (3)	6557 (3)	29 (1)
O(3)	4427 (2)	2176 (3)	3125 (3)	27 (1)
O(4)	4650 (3)	3611 (3)	844 (3)	27 (1)
O(5)	6761 (2)	2831 (2)	6063 (3)	18 (1)
O(6)	6404 (2)	3786 (3)	3408 (3)	17 (1)
O(7)	5136 (2)	646 (2)	1079 (3)	18 (1)
O(8)	6578 (2)	945 (3)	3815 (3)	20 (1)
C(1)	8984 (16)	1818 (22)	5675 (12)	27 (4)
C(2)	9794 (6)	887 (9)	6436 (8)	45 (3)
C(3)	10964 (6)	1121 (11)	6604 (9)	58 (3)
C(4)	11280 (10)	2311 (16)	5987 (13)	61 (5)
C(5)	10480 (8)	3181 (13)	5232 (14)	76 (5)
C(6)	9292 (7)	2997 (10)	5034 (10)	55 (3)
C(1A)	8854 (33)	1861 (37)	5248 (26)	18 (7)
C(2A)	9703 (13)	2412 (20)	6476 (20)	50 (6)
C(3A)	10842 (18)	2561 (28)	6432 (43)	93 (15)
C(4A)	11116 (18)	2165 (22)	5213 (31)	49 (8)
C(5A)	10258 (17)	1642 (18)	4043 (23)	56 (8)
C(6A)	9138 (13)	1469 (14)	4061 (16)	33 (5)

^a Equivalent isotropic *U* defined as one-third of the trace of the orthogonalized U_{ij} tensor.

Table II. Selected Bond Lengths (Å) for $V_2O_4(C_6H_5AsO_3H) \cdot H_2O$

As(1)–O(2)	1.715 (3)	As(1)–O(5)	1.697 (3)
As(1)–O(8)	1.683 (2)	As(1)–C(1)	1.907 (20)
As(1)–C(1A)	1.881 (41)	V(1)–O(3)	1.598 (3)
V(1)–O(4)	2.067 (3)	V(1)–O(6)	1.957 (2)
V(1)–O(7)	1.965 (2)	V(1)–O(8)	2.011 (2)
V(1)–O(5B)	2.358 (3)	V(2)–O(1)	1.584 (3)
V(2)–O(7)	1.861 (2)	V(2)–V(2A)	2.953 (2)
V(2)–O(5A)	2.032 (2)	V(2)–O(6A)	1.743 (3)
V(2)–O(7A)	1.942 (3)	V(1A)–O(5)	2.358 (3)
V(2B)–O(5)	2.032 (2)	V(2B)–O(6)	1.743 (3)
V(2A)–O(7)	1.942 (3)		

monochromator, was used to collect 2810 diffraction maxima ($2\theta < 55^\circ$) from a black needle-shaped crystal of dimensions $0.2 \times 0.2 \times 0.6$ mm at 298 K. Of these, 2510 were unique, $R_{\text{int}} = 0.018$, and 2271 observed ($F > 3\sigma(F)$). No absorption correction was applied to the data ($\mu = 4.704$ mm⁻¹). The structure was solved by direct methods and refined by full-matrix least-squares methods. High residual electron density above and below the plane of the phenyl ring attached to arsenic was observed after location and refinement of all the non-hydrogen atoms, indicating some disorder. This disorder was modeled by refinement of two orientations of the phenyl group as rigid groups, the second related to the first by a rotation about the C1–As bond of 78° and a displacement of the group through an angle of 12.3° toward O(8). The refined occupancies of the different orientations were 0.68 and 0.32. For clarity, only the major orientation is shown in the figures. Vanadium, arsenic, and oxygen atoms were refined anisotropically to $R = 0.0377$, $R_w = 0.0477$, GOF = 1.53. The highest peak on the final difference Fourier map was 1.59 e⁻/Å³. All computations were performed using SHELXTL PLUS (Nicolet) on a MicroVAX II. The atomic coordinates and equivalent isotropic displacement coefficients are given in Table I and selected bond lengths in Table II.

Results

The structure of $V_2O_4(C_6H_5AsO_3H) \cdot H_2O$ consists of layers formed of pairs of edge-sharing VO_5 square pyramids linked through corner-sharing to VO_6 octahedra and AsO_3C tetrahedra. The layers undulate sinusoidally in the *b* direction, with phenyl groups extending up from one oxide layer interdigitating with phenyl groups extending down from the layer above, as shown in Figure 1. The resulting layer repeat distance is 11.507 (4) Å. Each of the phenyl

(7) Huan, G.; Jacobson, A. J.; Johnson, J. W.; Corcoran, E. W., Jr. *Chem. Mater.* 1990, 2, 91–93.

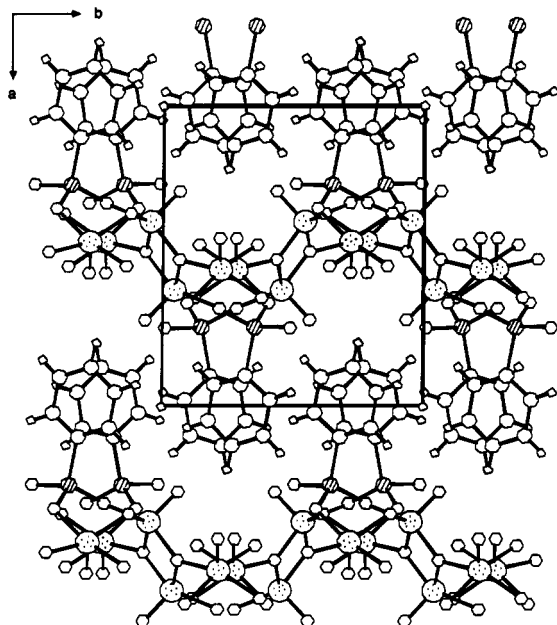


Figure 1. View of the *ab* plane of $V_2O_4(C_6H_5AsO_3H) \cdot H_2O$ showing the vanadium/phosphorus oxide layer separated by an interdigitating monolayer of phenyl groups. Vanadium atoms are stippled and arsenic atoms are cross-hatched.

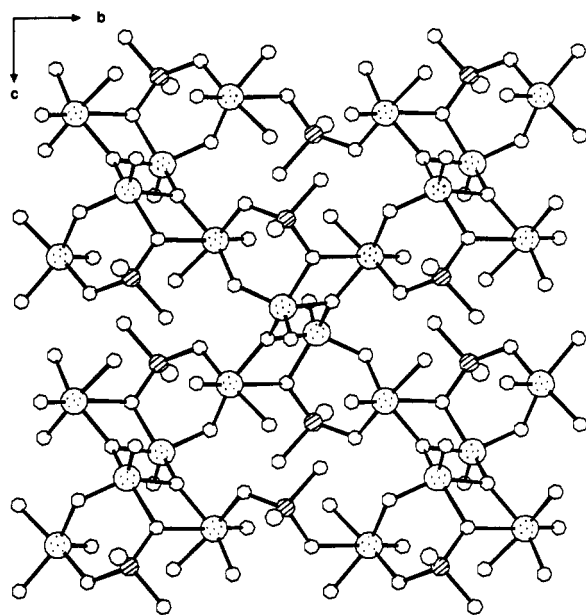


Figure 2. View of the *bc* plane of $V_2O_4(C_6H_5AsO_3H) \cdot H_2O$ illustrating the connectivity of the VO_5 square pyramids, the VO_6 octahedra, and the AsO_3C tetrahedra. Vanadium atoms are stippled and arsenic atoms are cross-hatched. The five carbon atoms of the phenyl group not attached to arsenic have been omitted for clarity.

groups is anchored to the layer by an As–C covalent bond, with the phenyl carbon atom occupying the fourth coordination site of each arsonate tetrahedron. The oxide layer, shown in Figures 2 and 3 with the phenyl groups omitted for clarity, contains pairs of edge-sharing vanadium square pyramids that are related by a crystallographic inversion center. The five-coordinate V(2) atom has an unshared oxygen atom in the apical position with a V(2)=O(1) distance of 1.584 (3) Å. It is bridged to its neighboring V(2) atom in the edge-sharing pair by two symmetry-related O(7) oxide ions at 1.861 (2) and 1.942 (3) Å. The V(2)–V(2) distance within the pair is 2.953 (2) Å. The coordination sphere of V(2) is completed by an oxide ion (O(6)) that bridges to V(1) at a distance of 1.743

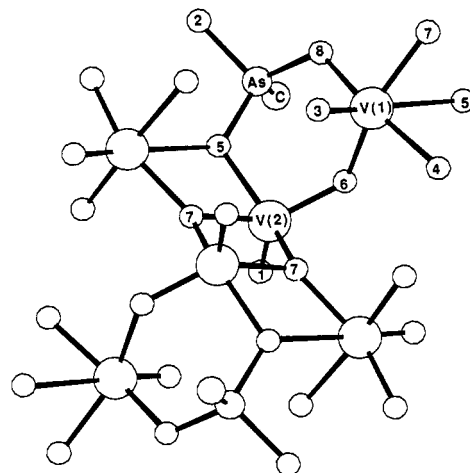


Figure 3. View of the *bc* plane of $V_2O_4(C_6H_5AsO_3H) \cdot H_2O$ as in Figure 2, expanded to show the atom labeling. Oxygen atoms are marked with numbers only.

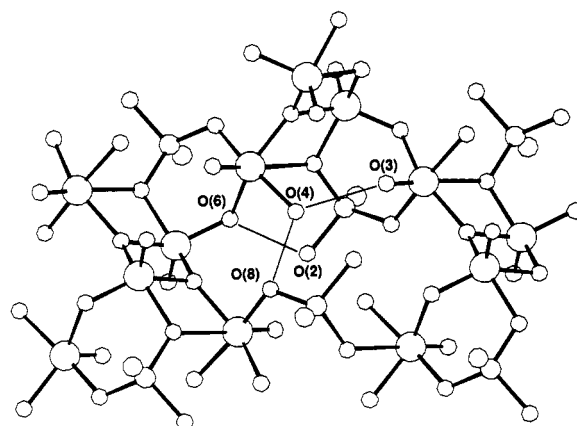


Figure 4. View of the *bc* plane of $V_2O_4(C_6H_5AsO_3H) \cdot H_2O$ as in Figure 2, expanded to show the intralayer hydrogen bonding.

Table III. Bond Valences of Vanadium Atoms in $V_2O_4(C_6H_5AsO_3H) \cdot H_2O$

V(1)		V(2)	
r_{V-O} , Å	s^a	r_{V-O} , Å	s^a
O(3)	1.598	O(1)	1.584
O(4)	2.067	O(5)	2.032
O(5)	2.358	O(6)	1.743
O(6)	1.957	O(7)	1.861
O(7)	1.965	O(7)'	1.942
O(8)	2.011		

$$\sum s_{V(1)} = 4.085$$

$$\sum s_{V(2)} = 4.955$$

^a Bond valence $s = \exp[-(r - r_0)/b]$ where r_0 and b for vanadium are 1.790 Å and 0.319.

(3) Å and an oxygen atom (O(5)) from the arsonate group at 2.032 (2) Å. Bond valence calculations clearly identify the five-coordinate V(2) atom as pentavalent and the octahedral V(1) atom as tetravalent, as shown by the results in Table III.⁸ The octahedrally coordinated V(1) atom exhibits the distortions typical for V^{4+} . There is an unshared vanadyl oxygen atom (O(3)) at 1.598 (3) Å, equatorial oxygen atoms at distances from 1.957 (2) to 2.067 (3) Å, and an O(5) atom in the position trans to the vanadyl oxygen atom at 2.358 (3) Å. The equatorial coordination sites are occupied by an O(8) atom from an arsonate group, O(6) and O(7) oxide ions from separate V(2) pairs, and a

(8) Brown, I. D. In *Structure and Bonding in Crystals*; O'Keefe, M., Navrotsky, A., Eds.; Academic Press: New York, 1981; Vol. II, Chapter 14.

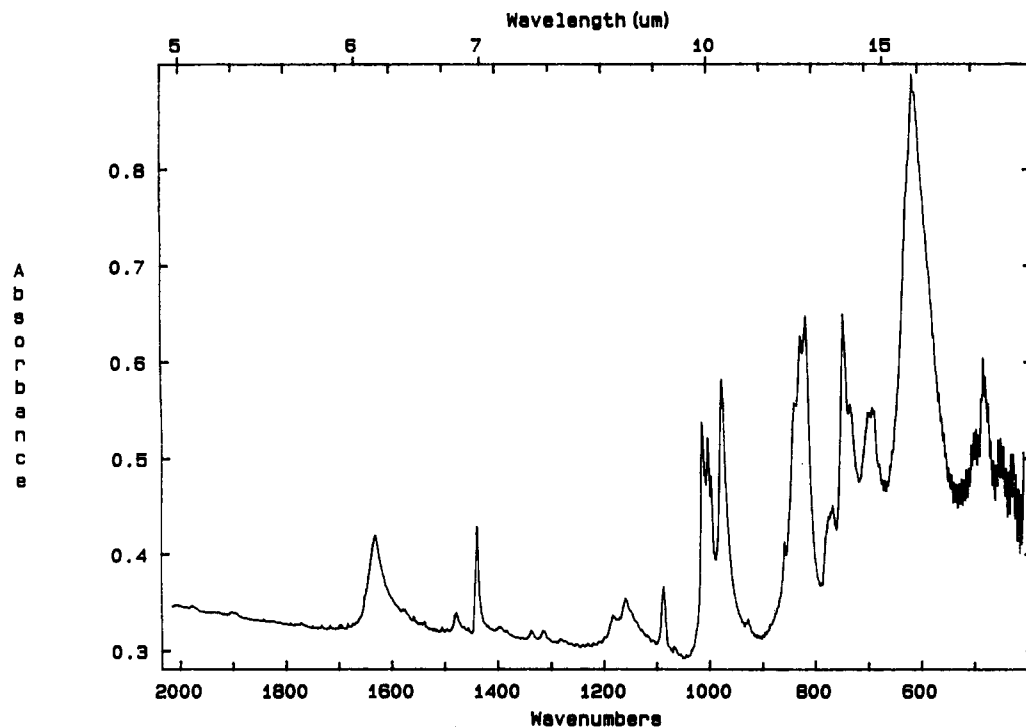


Figure 5. FTIR spectrum (solid KBr pellet) of $V_2O_4(C_6H_5AsO_3H) \cdot H_2O$.

water molecule (O(4)). Oxygen atoms in the structure exhibit coordination numbers from one to three. O(1) and O(3) are singly coordinated vanadyl oxygens, O(2), O(6), and O(8) are two coordinate, and O(4), O(5), and O(7) are three coordinate with O(2) being part of a hydroxyl group and O(4) a water molecule.

In addition to the vanadium–oxygen–arsenic covalent bonding network that holds the layers together in two dimensions, there are intralayer hydrogen bonds involving the phenylarsonate hydroxyl group and the coordinated water molecule. Although the hydrogen atoms could not be located from the diffraction data, hydrogen bonds as shown in Figure 4 can be identified by O...O contacts of 2.694 (Å) between the hydroxyl group O(2) and the O(6) ion and by contacts of 2.760 and 2.723 Å between the water molecule O(4) and the O(3) vanadyl oxygen atom and the O(8) arsonate oxygen atom.

The IR spectrum in the range 400–2000 cm^{-1} of the title compound is shown in Figure 5. The bands at 1632 cm^{-1} and from 1500 to 1050 cm^{-1} correspond to coordinated water and the phenylarsonate group, respectively. The bands at 1014, 1000, and 976 cm^{-1} are most likely V=O stretches with the lowest frequency corresponding to V(IV)=O. An absorption in pure phenyl arsonic acid is observed at 1000 cm^{-1} and may also contribute to the spectrum in this region.

The magnetic susceptibility of $V_2O_4(C_6H_5AsO_3H) \cdot H_2O$ is plotted as a function of temperature in Figure 6. The susceptibility increases as the temperature is lowered, typical of a paramagnetic system, but at 16 K it reaches a maximum and starts to decline due to antiferromagnetic interactions. In the temperature range 50–350 K the susceptibility obeys the Curie–Weiss law, $(\chi - \chi_0)^{-1} = (C - \Theta)/T$, with the diamagnetic contribution $\chi_0 = -4.075 \times 10^{-7}$ g/cm³, $C_g = 8.385 \times 10^{-4}$ g/(cm³ K), and $\Theta = -9.5$ K. The fit in this temperature range is excellent, as is demonstrated by the close comparison of the diamagnetic contribution derived from the fit with that calculated from Pascal's constants, -4.29×10^{-7} g/cm³. The μ_{eff} calculated from the Curie constant is 1.61 μ_B per formula unit, close to the spin-only value of 1.71 μ_B for one unpaired electron,

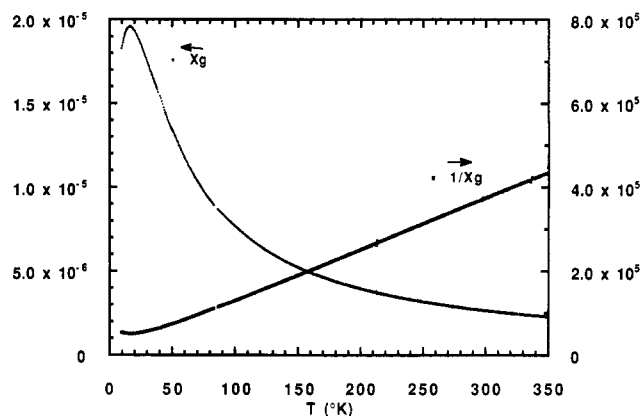


Figure 6. Magnetic susceptibility and its inverse as a function of temperature of $V_2O_4(C_6H_5AsO_3H) \cdot H_2O$.

indicating one unpaired spin for two vanadium atoms. According to the results of the structural analysis and the bond valence calculations, the unpaired spin resides on the six-coordinate vanadium atom V(1). These V(1) atoms are connected to each other within the layer indirectly through four-bond pathways involving single five-coordinate d⁰ V(2) atoms, through four-bond pathways involving phenylarsonate groups, and through six-bond pathways involving both atoms in the V(2) pairs. A detailed description of the antiferromagnetic exchange interactions requires inclusion of these potential exchange pathways.

Conclusions

The mixed valence compound $V_2O_4(C_6H_5AsO_3H) \cdot H_2O$ has been isolated by hydrothermal synthesis and structurally characterized. The compound is remarkably different from the analogous $VOC_6H_5PO_3 \cdot H_2O$ phase prepared under very similar conditions which contains only V(IV). Both compounds contain V=O groups, but in the phosphonate, all of the other oxygen atoms are shared between both phosphorus and vanadium atoms. In contrast, the arsonate phase contains oxygen atoms shared between vanadium atoms only and an unionized As–OH

group. The simultaneous presence of basic oxide atoms and an unionized acidic hydroxyl is unusual but is generally consistent with V-O-As bonds being weaker than V-O-P bonds as suggested by the higher solubilities observed for vanadium arsenates compared with those of vanadium phosphates. The effect of intralayer hydrogen bonding and steric factors associated with packing the phenyl groups in the interlayer space must also be important in determining the final composition and structure. Further comparative studies of vanadyl organo-

phosphonate and arsonate structures are in progress.

Acknowledgment. We thank D. P. Goshorn for the magnetic susceptibility measurements.

Registry No. $V_2O_4(C_6H_5AsO_3H) \cdot H_2O$, 130063-84-2; $C_6H_5AsO_3H_2$, 98-05-5; V_2O_5 , 1314-34-7.

Supplementary Material Available: Tables of anisotropic thermal parameters, bond angles, and hydrogen atom coordinates (2 pages); observed and calculated structure factors (9 pages). Ordering information is given on any current masthead page.

Magnetic Exchange Interactions in One-Dimensional Copper(II) Compounds

Pere Alemany and Santiago Alvarez*

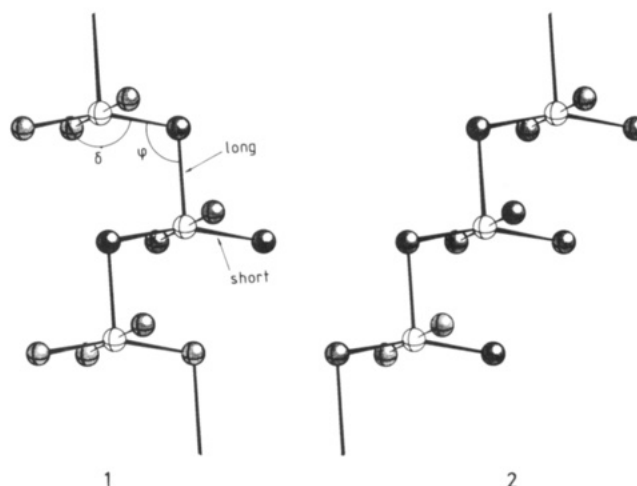
Departament de Química Inorgànica, Universitat de Barcelona, Diagonal 647, 08028 Barcelona, Spain

Received June 8, 1990

A theoretical study is presented of the weak magnetic exchange interaction in one-dimensional halo-bridged pentacoordinate Cu(II) complexes with $CuY_3(\mu-X)$ and $CuY_2(\mu-X)_2$ cores for the repeat unit ($X = Cl, Br$), in which the arrangement of the ligands around the copper atoms can vary from trigonal bipyramidal to square pyramidal to pseudooctahedral. Electronic band structure calculations of the extended Hückel type were performed on the model chain compounds $[CuCl_3(\mu-Cl)]_n^{2-}$, $[CuBr_3(\mu-Br)]_n^{2-}$, and $[CuCl_2(\mu-Cl)_2]_n^{2-}$, and the dependence of the bandwidth (W) of the highest occupied band on the structural parameters is studied. The largest values of W occur for the trigonal-bipyramidal geometry and a large Cu-bridge-Cu angle ($\varphi \sim 180^\circ$), whereas W is practically constant and small for a square pyramid and small bridging angles, in good qualitative agreement with the experimental coupling constants.

The study of magnetic exchange interactions between transition-metal ions in dimers and in chains has been an area of constant interest during the past two decades.¹ Copper(II) complexes, with one unpaired electron per copper atom, provide the simplest case study, yet the geometries available to such complexes make them a rich field for both experimental and theoretical research.

A particular case of Cu(II) chain complexes showing weak magnetic coupling is that of halo-bridged pentacoordinate complexes with $CuY_3(\mu-X)$ or $CuY_2(\mu-X)_2$ cores for the repeat unit ($X = Cl, Br$). In the singly bridged chains, long Cu-X bonds occupy either the apical position of a square pyramid or one of the equatorial sites of a trigonal bipyramid,²⁻⁶ with an idealized local symmetry C_{2v} around the Cu atom. The geometrical parameters that define such structures are shown in 1: an angle δ of $\sim 180^\circ$ corresponds to a square pyramid with the bridging ligand coordinated to neighboring copper atoms in axial (longer Cu-Cl bond distance) and equatorial positions, respectively. A value of $\delta \sim 120^\circ$, on the other hand, corresponds to a trigonal bipyramid with the bridging ligand occupying



equatorial positions of two copper atoms. The bridging angle φ is also found to vary in the range $114-145^\circ$. Notice that in 1 there are two Cu atoms per repeat unit. For linear chains 2, with one Cu per unit cell⁷⁻⁹ both angles are related through the equation $\delta = 360^\circ - 2\varphi$.

A particular situation occurs when $\varphi \approx 90^\circ$ and $\delta \approx 180^\circ$ in structures 1 and 2. Then, the ligand under the equa-

(1) Willett, R. D.; Gatteschi, D.; Kahn, O., Eds. *Magneto-Structural Correlations in Exchange Coupled Systems*; D. Reidel: Dordrecht, 1985.

(2) Bream, R. A.; Estes, E. D.; Hodgson, D. J. *Inorg. Chem.* **1975**, *14*, 1672.

(3) Lundberg, B. K. S. *Acta Chem. Scand.* **1972**, *26*, 3977.

(4) Willett, R. D.; Chang, K. *Inorg. Chim. Acta* **1970**, *4*, 447.

(5) Watkins, N. T.; Jeter, D. Y.; Hatfield, W. E.; Horner, S. M. *Trans. Faraday Soc.* **1971**, *67*, 2431.

(6) Bandoli, G.; Biagini, M. C.; Clemente, D. A.; Rizzardi, G. *Inorg. Chim. Acta* **1976**, *20*, 71.

(7) Sheldrick, W. S.; Bell, P. Z. *Naturforsch.* **1987**, *42b*, 195.

(8) Rojo, T.; Mesa, J. L.; Arriortua, M. I.; Savariault, J. M.; Galy, J.; Villeneuve, G.; Beltrán, D. *Inorg. Chem.* **1988**, *27*, 3904.

(9) Folgado, J. V.; Coronado, E.; Beltrán, D.; Burriel, R.; Fuentès, A.; Miravittles, C. J. *Chem. Soc., Dalton Trans.* **1988**, 3041.